Low-density lipoprotein receptor overexpression enhances the rate of brain-to-blood Aβ clearance in a mouse model of β-amyloidosis

Joseph M. Castellano[a], Rashid Deane[b], Andrew J. Gottesdiener[a], Philip B. Verghese[a], Floy R. Stewart[a], Tim West[c], Andrew C. Paoletti[c], Tristan R. Kasper[b], Ronald B. DeMattos[d], Berislav V. Zlokovic[e], and David M. Holtzman[a,f,1]

[a]Department of Neurology, Hope Center for Neurological Disorders, Charles F. and Joanne Knight Alzheimer's Disease Research Center, and [f]Department of Developmental Biology, Washington University School of Medicine, St. Louis, MO 63110; [b]Department of Neurosurgery, Center for Translational Neuromedicine, University of Rochester Medical Center, Rochester, NY 14642; [c]C2N Diagnostics, Center for Emerging Technologies, St. Louis, MO 63108; [d]Lilly Research Labs, Eli Lilly and Co., Indianapolis, IN 46285; and [e]Department of Physiology and Biophysics, Zilkha Neurogenetic Institute, University of Southern California Keck School of Medicine, Los Angeles, CA 90089

Edited by Thomas C. Südhof, Stanford University School of Medicine, Stanford, CA, and approved August 7, 2012 (received for review April 19, 2012)

The apolipoprotein E (*APOE*)-ε4 allele is the strongest genetic risk factor for late-onset, sporadic Alzheimer's disease, likely increasing risk by altering amyloid-β (Aβ) accumulation. We recently demonstrated that the low-density lipoprotein receptor (LDLR) is a major apoE receptor in the brain that strongly regulates amyloid plaque deposition. In the current study, we sought to understand the mechanism by which LDLR regulates Aβ accumulation by altering Aβ clearance from brain interstitial fluid. We hypothesized that increasing LDLR levels enhances blood–brain barrier-mediated Aβ clearance, thus leading to reduced Aβ accumulation. Using the brain Aβ efflux index method, we found that blood–brain barrier-mediated clearance of exogenously administered Aβ is enhanced with LDLR overexpression. We next developed a method to directly assess the elimination of centrally derived, endogenous Aβ into the plasma of mice using an anti-Aβ antibody that prevents degradation of plasma Aβ, allowing its rate of appearance from the brain to be measured. Using this plasma Aβ accumulation technique, we found that LDLR overexpression enhances brain-to-blood Aβ transport. Together, our results suggest a unique mechanism by which LDLR regulates brain-to-blood Aβ clearance, which may serve as a useful therapeutic avenue in targeting Aβ clearance from the brain.

dementia | low-density lipoprotein-related protein 1 | peripheral | in vivo microdialysis | sequestration

Accumulation of soluble amyloid-β (Aβ) into toxic oligomers and amyloid plaques is widely hypothesized to initiate a pathogenic cascade leading to synaptic dysfunction, neuronal death, and, ultimately, loss of cognitive function (1–3). The factors that initiate or regulate risk and onset of Aβ accumulation in sporadic, late-onset Alzheimer's disease (AD) cases that account for the majority of total cases remain poorly understood. Emerging evidence suggests that faulty clearance from the brain accounts for Aβ accumulation in sporadic, late-onset AD (4). The strongest identified genetic risk factor for this disease is the *APOE* ε4 allele, which increases AD risk and decreases onset by 10–15 y in a dose-dependent fashion (reviewed in ref. 5). *APOE* status is hypothesized to modulate AD risk and age of onset by regulating the onset of amyloid deposition (6–11). Using a mouse model that develops human apoE isoform-dependent β-amyloidosis (12), we recently provided direct in vivo evidence that human apoE isoforms differentially regulate soluble Aβ clearance from brain interstitial fluid (ISF) (11), strongly suggesting that *APOE*'s role in AD risk development is related to its regulation of Aβ clearance pathways.

Aβ is eliminated from brain ISF through various routes, including cellular uptake and degradation, ISF bulk flow, and blood–brain barrier (BBB)-mediated transport. ApoE has been shown to impede the clearance of Aβ across the BBB (13–15), and various members of the low-density lipoprotein receptor (LDLR) family have been implicated in mediating apoE-independent or apoE-dependent Aβ clearance across the BBB. Although low-density lipoprotein receptor-related protein 1 (LRP1) has been well characterized for its role in BBB-mediated Aβ clearance (13–15), whether LDLR plays a role in Aβ clearance across the BBB is unclear. Recent studies have identified LDLR as a major central nervous system (CNS) apoE receptor that regulates amyloid deposition in various mouse models of β-amyloidosis (16–19). Although we demonstrated that LDLR overexpression decreases amyloid deposition by altering the steady-state concentration of Aβ in the ISF (18), the mechanism by which LDLR regulates ISF Aβ metabolism remains to be characterized. To this end, we used the brain efflux index (BEI) method to demonstrate a unique role for LDLR in BBB-mediated Aβ clearance. To directly compare the rate that Aβ enters blood from the brain, we first created mice that express Aβ solely within the brain with and without LDLR overexpression. We then used an anti-Aβ antibody to capture endogenously produced, brain-derived Aβ in the blood of these mice, revealing that LDLR overexpression increases the rate that Aβ enters blood from the brain.

Results

In young wild-type [nontransgenic (NTG)] or LDLR-TG [transgenic (TG)] mice (18), we used the BEI method (13–15, 20) to test the hypothesis that LDLR regulates steady-state Aβ levels by enhancing clearance from the brain. To compare the clearance kinetics from the brain over various time points (15–150 min), 12 nM [^{125}I]-radiolabeled, monomeric Aβ40 was injected simultaneously with [^{14}C]inulin into brain ISF. Unlabeled and radiolabeled Aβ have been shown to exhibit nearly identical clearance kinetics (13). [^{14}C]inulin serves as a reference marker of ISF bulk flow because it does not actively clear across the BBB. Total brain ISF Aβ clearance, corrected for degradation within the brain (*SI Materials and Methods*), was significantly faster from brains of

Author contributions: J.M.C., B.V.Z., and D.M.H. designed research; J.M.C., R.D., A.J.G., P.B.V., F.R.S., T.W., A.C.P., and T.R.K. performed research; R.B.D. contributed new reagents/analytic tools; J.M.C., R.D., A.J.G., P.B.V., T.W., and D.M.H. analyzed data; and J.M.C. and D.M.H. wrote the paper.

Conflict of interest statement: D.M.H. cofounded C2N Diagnostics. Some measurements of samples were assessed by employees of C2N Diagnostics. D.M.H. is on the scientific advisory boards of Satori and En Vivo, and consults for Pfizer, Bristol-Myers Squibb, and Innogenetics.

This article is a PNAS Direct Submission.

[1]To whom correspondence should be addressed. E-mail: holtzman@neuro.wustl.edu.

This article contains supporting information online at www.pnas.org/lookup/suppl/doi:10.1073/pnas.1206446109/-/DCSupplemental.

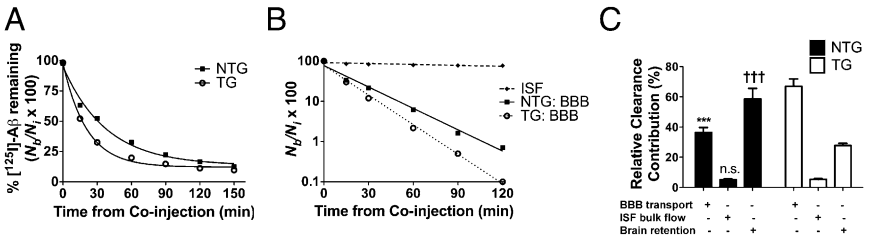

Fig. 1. LDLR enhances clearance of radiolabeled Aβ from brain. (*A*) Percentage remaining for 12 nM [^{125}I]Aβ40 microinjected in ISF of caudate-putamen in NTG (■) and TG (○) mice killed at various time points. Percentage recovery was calculated from Eq. **S1** (*SI Materials and Methods*). (*B*) Time-dependent clearance of [^{125}I]Aβ40 by passive ISF bulk flow (♦) and across the BBB after correction for degradation within brain by TCA precipitation method (NTG, ■; TG, ○) calculated from data in Fig. 1*A* and Eq. **S4** (*SI Materials and Methods*). (*C*) Using fractional rate constants calculated in Table S1, relative contributions of degradation-corrected clearance of [^{125}I]Aβ40 by the BBB and ISF bulk flow, as well as retention within brain, were calculated for NTG (black bars) and TG (white bars) mice. Each component is indicated with a plus sign (+). Complete time course includes 32–41 mice (n = 4–6 mice per time point for each group). Values in *A* and *C* are represented as mean ± SEM. When two-way ANOVA was significant (with genotype and component as factors), differences among clearance components were assessed using Tukey's post hoc test for multiple comparisons. ***$P < 0.001$, % BBB for NTG vs. TG. $^{\dagger\dagger\dagger}P < 0.001$, % brain retention for NTG vs. TG. n.s., no significant difference between ISF bulk flow components between NTG and TG.

TG mice compared with NTG mice (Fig. 1*A*; see Fig S1*A* for scatterplot of data). Analysis of major components of brain-to-blood efflux (BBB and ISF bulk flow) revealed that LDLR overexpression increased the BBB-mediated component of Aβ clearance compared with NTG mice, as indicated by the greater slope for TG vs. NTG mice from a plot of [^{125}I]Aβ40 remaining vs. time (Fig. 1*B*). Notably, the contribution of ISF bulk flow to total Aβ clearance was minimal (Fig. 1*B*), consistent with previous studies (14, 15, 20). Given the purported role of apoE in BBB integrity (21, 22), we monitored the elimination of [^{14}C]inulin over the entire time course for both groups, which revealed that [^{14}C]inulin was cleared in a slow, passive manner and to a similar extent in both groups (Fig. S1*B*), strongly suggesting an intact BBB in TG mice.

Based on the passive elimination kinetics of inulin from brain ISF and the total clearance of [^{125}I]Aβ40, we used our kinetic model (*SI Materials and Methods*) to calculate the relative contribution of ISF bulk flow and BBB transport to Aβ clearance in NTG and TG mice (Fig. 1*C*). A greater proportion of total Aβ clearance was attributed to BBB transport in TG mice compared with NTG mice (66.9% compared with 36.3%; Fig. 1*C*). Conversely, less Aβ was retained within brains of TG mice compared with NTG mice (27.8% compared with 58.6%, respectively). The proportion of Aβ clearance attributed to ISF bulk flow did not differ between NTG and TG mice (5.1% compared with 5.3%, respectively). Fractional rate constants (k, min^{-1}) were calculated (*SI Materials and Methods*) to determine the rates of Aβ clearance mediated by the BBB, ISF bulk flow, and brain retention (Table S1). We performed trichloroacetic acid (TCA) precipitation for brains of each group at early (30 min) and late (120 min) time points to compare cellular degradation within the remaining fraction of brain [^{125}I]Aβ. The proportion of TCA-precipitable (intact) Aβ did not differ significantly between NTG and TG mice, although a trend was noted toward greater degradation in brains of TG mice at both time points (Fig. S1*C*). Together, these results suggest LDLR enhances BBB-mediated Aβ clearance, whereas other modes of clearance do not appear to be significantly altered. Surprisingly, although LDLR overexpression clearly increased BBB-mediated clearance of [^{125}I]Aβ, expression of the HA-tagged LDLR transgene did not overlap with expression of BBB markers such as CD31 [platelet endothelial cell adhesion molecule (PECAM-1)] (Fig. S2*A*) (23), nor did it colocalize with aquaporin 4 (Aqp4) expression (Fig. S2*B*), which labels microvessel abluminal surfaces at the astrocyte-vessel interface (24). These results suggest the LDLR overexpression in neurons and astrocytes (18) likely increases BBB-mediated Aβ clearance through an indirect mechanism involving other apoE receptors at the BBB, such as LRP1—a receptor shown to directly mediate Aβ clearance across the BBB (14, 15, 26). To test this hypothesis, we delivered an anti-LRP1 antibody (N20) or vehicle into the brains of TG mice immediately before coinjection of 12 nM [^{125}I]Aβ40 and [^{14}C]inulin. Blocking LRP1 resulted in a dramatic attenuation of the BBB component of Aβ clearance in TG mice compared with vehicle (Fig. S3). Though blocking LRP1 led to decreased BBB transport and thus greater brain retention, the proportion of Aβ cleared via ISF bulk flow was unaltered compared with vehicle. Together, these results suggest that the increased BBB component of Aβ clearance observed with LDLR overexpression is, in part, mediated by the action of LRP1 at the BBB.

The rapid degradation of Aβ in the periphery ($t_{1/2}$ = 2–3 min) precludes a direct and sensitive measurement of the rate of Aβ appearance from brain into blood (27, 28). To more directly assess the rate of brain-to-blood Aβ clearance, we first cross-bred LDLR-TG mice with the PDAPP (APP-V717F) mouse model of β-amyloidosis. PDAPP mice have been previously reported to produce human APP/Aβ solely within the CNS (29, 30), allowing the fate of Aβ to be followed from brain into blood. Hippocampus and cortex from 10-mo-old PDAPP/LDLR mice (PD-TG) exhibited 2.7-fold and 4.8-fold less Aβ burden, respectively, compared with PDAPP (PD-NTG) littermates (Fig. 2 *A* and *B*). Fibrillar amyloid burden in these regions was also significantly reduced as a result of LDLR overexpression (Fig. 2 *C* and *D*). Additionally, LDLR overexpression decreased apoE levels in hippocampal and cortical homogenates by 2.9-fold and 2.5-fold, respectively, compared with mice expressing normal levels of LDLR (Fig. 2*E*), further validating these mice as a useful model to understand the role of LDLR in brain-to-blood clearance of centrally derived human Aβ.

To directly compare the rate at which Aβ enters the blood from brain in PD-NTG and PD-TG mice, we developed a method to capture centrally derived, endogenously secreted Aβ over time in the periphery, thus protecting it from rapid degradation. Based on work characterizing the ability of anti-Aβ antibodies to rapidly bind Aβ in the periphery and prolong its half-life (30–32), we identified an anti-Aβ antibody specific for the central domain of Aβ (HJ5.1) that strongly bound Aβ40 and Aβ42 with thermodynamic dissociation constants (K_ds) of 20.8 ± 5.45 nM and 0.623 ± 0.230 nM, respectively (Fig. S4). Consistent with the long half-life of antibodies in the periphery (30), the plasma concentration of biotinylated HJ5.1 i.v. injected in PDAPP mice was stable over the entire serial retro-orbital plasma collection period and was in significant molar excess of circulating Aβ (Fig. 3*A*). Only a small fraction of injected antibody was found in hippocampal and cortical homogenates (2.65×10^{-3}% to 1.75×10^{-2}%; Table S2). To assess whether this small fraction alters brain Aβ metabolism, and to test whether HJ5.1 present in the periphery alters the brain-to-blood equilibrium of Aβ efflux over

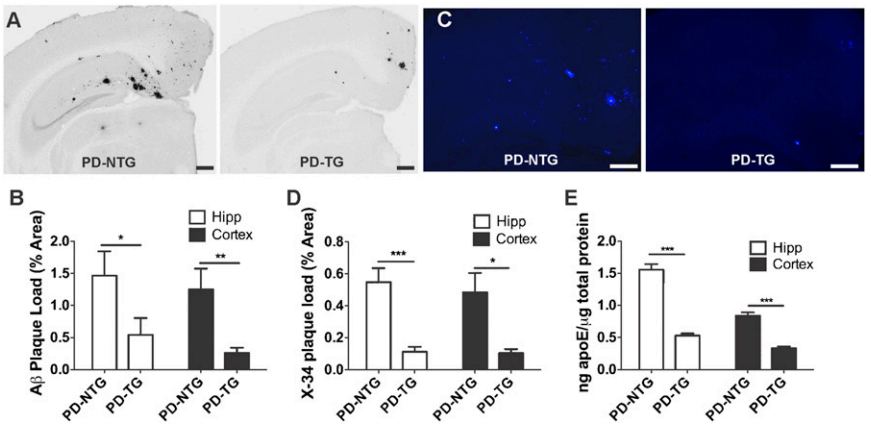

Fig. 2. LDLR overexpression in PDAPP mice markedly decreases brain Aβ/amyloid deposition and apoE levels. (*A*) Representative coronal brain sections from 10-mo-old, sex-matched PDAPP$^{+/-}$ mice expressing normal levels of LDLR (PD-NTG), and PDAPP$^{+/-}$ mice overexpressing LDLR (PD-TG). Aβ immunostaining was performed using anti-Aβ antibody (biotinylated 3D6). (Scale bars, 300 μm.) (*B*) Quantification of the area of the hippocampus or cortex occupied by Aβ immunostaining ($n = 9$ mice per group). (*C*) Representative amyloid burden in coronal brain sections from 10-mo-old, sex-matched PD-NTG mice and PD-TG mice. Amyloid was visualized using the congophilic fluorescent dye, X-34. (Scale bars, 100 μm.) (*D*) Quantification of the area of hippocampus or cortex occupied by X-34 staining ($n = 9$–10 mice per group). In *B* and *D*, groups were compared using the Mann–Whitney *U* test. $^{*}P < 0.05$, $^{**}P < 0.01$, $^{***}P < 0.001$. (*E*) ApoE protein levels measured by sensitive sandwich ELISA in hippocampal and cortical homogenates from PD-NTG and PD-TG mice (at 3–4 mo of age to avoid confounding effects from amyloid plaque deposition; $n = 9$ mice per group). Differences between groups were assessed using two-tailed Student's *t* test (with Welch's correction for *E*). $^{***}P < 0.001$. Values represent means ± SEM.

this acute time course (30), we sampled brain ISF during in vivo microdialysis in PD-NTG mice injected with HJ5.1. Levels of ISF Aβ over a 5-h period following i.v. antibody administration did not change compared with baseline ISF Aβ levels (Fig. 3 *B* and *C*). ISF Aβ metabolism was similarly unchanged following HJ5.1 injection in PD-TG mice (Fig. 3 *D* and *E*), arguing that administration of HJ5.1 would not confound brain-to-blood Aβ efflux by differentially altering Aβ metabolism in the brains of either group of mice. Notably, PDAPP mice overexpressing LDLR exhibited markedly lower steady-state ISF Aβ levels before HJ5.1 administration compared with PD-NTG mice (Fig. 3*F*), consistent with decreased Aβ accumulation observed in older PD-TG mice compared with PD-NTG mice. To compare the rate of brain-to-blood Aβ appearance in both groups of mice, we collected retro-orbital blood samples serially at various time points from mice of both groups following i.v. HJ5.1 administration. The concentration of CNS-derived human Aβ in plasma samples was determined using quantitative mass spectrometry. The kinetics of Aβ appearance were reliably linear for the duration of the time course in each mouse (Fig. 4*A*), reflecting the rapid capture of human Aβ entering the periphery from brain. The plasma appearance rate of human Aβ was significantly faster in PD-TG mice compared with PD-NTG mice (92 ± 4.8 pg·mL^{-1}·min^{-1} vs. 69 ± 6.9 pg·mL^{-1}·min^{-1}; Fig. 4*B*). These results directly demonstrate in vivo that LDLR regulates the rate at which endogenously produced Aβ enters the blood from brain.

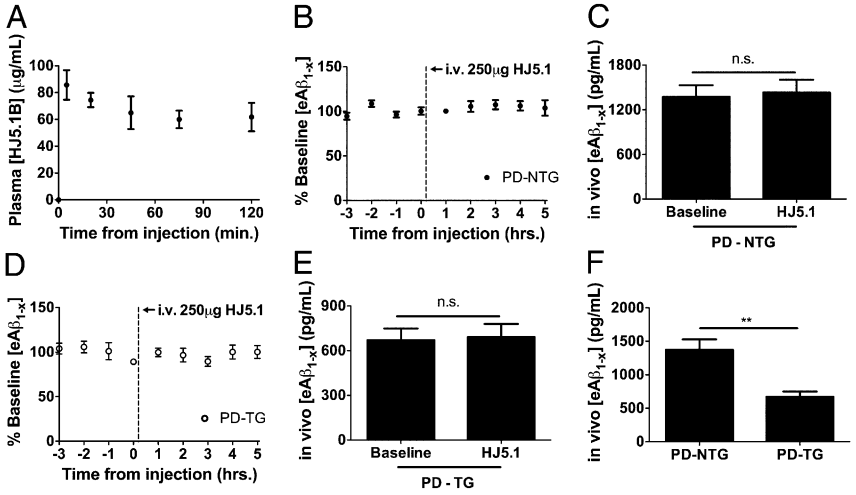

Fig. 3. Intravenous HJ5.1 administration results in stable antibody steady-state levels in plasma without altering brain ISF Aβ metabolism. (*A*) Concentration of biotinylated HJ5.1 (HJ5.1B) in plasma collected by serial retro-orbital bleeds following intrajugular injection of HJ5.1B in PDAPP$^{+/-}$ mice ($n = 4$; 3–4 mo old). (*B*) In vivo microdialysis was performed in PDAPP$^{+/-}$ mice expressing normal levels of LDLR (PD-NTG) to monitor ISF $A\beta_{1-x}$ levels during baseline sampling as well as the period following intrajugular administration of 250 μg HJ5.1 ($n = 5$; 3–4 mo old). (*C*) Mean effect of HJ5.1 treatment on ISF $A\beta_{1-x}$ levels compared with mean baseline period preceding treatment. (*D* and *E*) Experiments in *B* and *C* were repeated in PDAPP$^{+/-}$ mice overexpressing LDLR (PD-TG) ($n = 5$; 3–4 mo old). (*F*) ISF $A\beta_{1-x}$ levels during the baseline period of microdialysis were compared between PD-NTG and PD-TG mice. Differences between groups were assessed by paired Student's *t* test in *C* and *E* and Student's *t* test in *F*. $^{**}P < 0.01$. Values represent mean ± SEM.

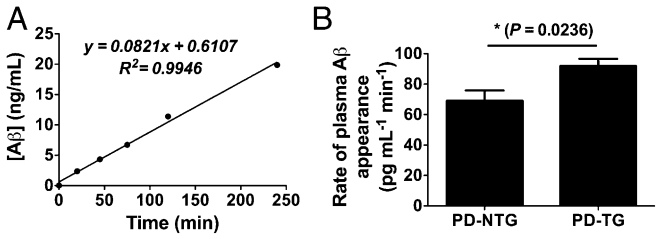

Fig. 4. Antibody-assisted plasma accumulation of brain Aβ reveals faster brain-to-blood appearance rate in PDAPP mice overexpressing LDLR. (*A*) Representative plasma accumulation experiment illustrating kinetics of brain-derived Aβ appearance in plasma collected by serial retro-orbital bleeds following HJ5.1 treatment. Appearance rates were calculated from the slopes of individual linear regressions, e.g., for *A*, 82.1 pg·mL^{-1}·min^{-1}. (*B*) Mean rate of Aβ appearance in PDAPP$^{+/-}$ mice expressing normal levels of LDLR (PD-NTG) or PDAPP$^{+/-}$ mice overexpressing LDLR (PD-TG) (n = 6–7 per group; 3.5–4.5 mo old). Difference between groups was analyzed using two-tailed Student's t test. *$P < 0.05$. Values in *B* represent mean ± SEM.

Discussion

The accumulation of Aβ into high-order species and amyloid plaques throughout life is hypothesized to be a critical initiating event in AD pathogenesis (2, 3, 33). Recent data have emerged suggesting that Aβ accumulates in the vast majority of AD cases as a result of impaired Aβ clearance and not increased synthesis (4). We recently provided in vivo evidence that human apoE isoforms differentially regulate soluble Aβ clearance from brain ISF (11, 15), with the slowest Aβ clearance observed in mice expressing *APOE* ε4 (11), the strongest identified genetic risk factor for AD (5). Based on previous evidence that receptors for apoE modulate Aβ metabolism (34), we sought to elaborate the previously unappreciated role of LDLR in Aβ metabolism. Although LDLR is well-studied for its role in mediating removal of cholesterol and cholesterol esters in the periphery (35), little is known about its function in the CNS. Recent work has identified that LDLR is a major apoE receptor in the CNS (16) that profoundly affects the accumulation of Aβ (17–19). In the current study, we found that LDLR regulates clearance of exogenously administered Aβ across the BBB but does not significantly alter clearance by ISF bulk flow. We then created mice that overexpress LDLR in the setting of CNS expression of human Aβ using the PDAPP mouse model of β-amyloidosis. We found that LDLR overexpression in young PDAPP mice markedly decreases apoE levels and decreases Aβ deposition in aged PDAPP mice. We next developed a method to stabilize human Aβ entering the peripheral circulation from brain using a high-affinity anti-Aβ antibody. Using this method, we found that LDLR overexpression significantly increases the appearance rate of endogenously produced human Aβ from brain to blood. Together, our results suggest a mechanism whereby LDLR regulates brain Aβ accumulation via BBB-mediated elimination of brain Aβ.

Previous work has identified that several members of the LDLR family of receptors, including LRP1, LRP1B, SorLA, and apoER2, regulate the trafficking and processing of the amyloid precursor protein (APP) (34, 36–39). For example, LRP1 has been shown to interact with APP, regulating its internalization, trafficking, and its subsequent processing to Aβ (36, 40–42). We did not observe any changes in APP expression or processing in brains of mice overexpressing LDLR (18); our work strongly suggests that LDLR influences Aβ metabolism by affecting its clearance from the brain into blood, a mechanism previously suggested only for LRP1 and VLDLR (13–15, 26). ApoE has been shown to impede the clearance of Aβ from brain ISF (13, 15, 43); therefore, it is likely that the reduction of apoE levels with LDLR overexpression facilitates greater ISF Aβ clearance across the BBB. Given that LDLR overexpression was limited to neurons and astrocytes in our model (18), with no transgene expression in cells constituting the BBB (Fig. S2), we speculate that LDLR-mediated removal of extracellular apoE results in increased Aβ clearance across the BBB via LRP1, which has been implicated in mediating direct BBB-mediated Aβ clearance (14). Indeed, we provide evidence that LRP1 may be, in part, responsible for mediating Aβ clearance across the BBB in the context of LDLR overexpression by using an anti-LRP1 antibody approach coupled with the BEI method (Fig. S3). We speculate that the reduction in apoE concentration as a result of LDLR overexpression allows free Aβ in the ISF to clear more rapidly across the BBB via LRP1 and other receptors, given that apoE has been suggested to impair Aβ clearance (15, 43). Further studies are needed to elaborate the putative cross-talk between LDLR and other apoE receptors that governs ISF Aβ elimination from the brain. Moreover, though our data revealed only subtle trends toward greater Aβ degradation as a result of LDLR overexpression, we cannot rule out a role for LDLR in mediating Aβ degradation within particular cell types (44), the magnitude of which may have been too subtle to detect in whole-brain homogenates. Conditional deletion strategies targeting LDLR expression within particular CNS cell types will be useful to address these possibilities. Though the current study focused on murine apoE, our results demonstrate a role for LDLR in BBB-mediated Aβ clearance, warranting further investigation into the contribution of this clearance pathway to apoE isoform-dependent Aβ clearance. This regulation may be especially relevant given that the affinity of apoE for LDLR is related to apoE isoform (45, 46). Given that haploinsufficiency of either apoE3 or apoE4 leads to reduced amyloid burden (25, 47), we would expect that reducing apoE levels by LDLR overexpression may result in enhanced Aβ clearance across the BBB in the context of either apoE3 or apoE4, and that increasing apoE expression would impair clearance. Future experiments to assess this possibility will be useful as apoE-reducing strategies are considered for AD treatment and prevention.

Although an established method to examine different components of Aβ elimination, the BEI method uses a kinetic model that cannot perfectly describe the complex physiology of the BBB and other routes of efflux. Moreover, the rapid and widespread distribution of Aβ species throughout various peripheral spaces and compartments makes following the fate of radiolabeled Aβ into the blood difficult. Acknowledging these limitations, we sought to verify our observations with an independent method to assess brain-to-blood Aβ elimination. The rapid degradation of Aβ once it enters the blood from brain precludes direct and reliable measurement of its influx rate by conventional means (27, 28). Thus, we reasoned that an anti-Aβ antibody would bind CNS-derived Aβ within the blood, preventing its degradation to allow direct measurement of its appearance rate. We previously hypothesized that anti-Aβ antibody treatment in the periphery leads to a rapid rise in plasma Aβ, in part by altering the efflux of Aβ from the brain (30, 32). In the current study, our microdialysis results suggest that peripheral administration of the HJ5.1 (anti-Aβ$_{13–28}$) antibody does not alter the metabolism of Aβ within the brain in the acute phase (5 h) during which we analyzed Aβ influx into the circulation. Though it is possible that over longer periods of time (days to weeks), certain anti-Aβ antibodies may alter Aβ metabolism in the brain, this possibility was not assessed in these experiments. A recent study suggested that the anti-Aβ antibody, m266, alters Aβ metabolism in the CNS by entering the brain and sequestering soluble Aβ (49). The small fraction of antibody that entered the brain in our study did not alter Aβ levels in the ISF over a very short timeframe, perhaps a reflection of its lower affinity for Aβ compared with the m266 antibody. Alternatively, the microdialysis technique may be insensitive to identifying the initial altered equilibrium changes

in ISF Aβ. Importantly, our plasma accumulation results were consistent with results obtained using the BEI method (Fig. 1), further validating the BEI method as a useful technique to assess the contribution of different clearance components in overall Aβ clearance from the brain. Provided a suitable antibody is available that does not significantly alter brain Aβ metabolism, the plasma accumulation technique we report herein may be useful to screen drugs targeting Aβ elimination from brain to blood, while also serving as a useful tool for probing the biology of brain apoE receptors and their role in Aβ metabolism.

Our findings that LDLR regulates BBB-mediated Aβ clearance provide rationale for targeting apoE receptors in the brain, and specifically in brain endothelial cells, as an additional means to reducing Aβ accumulation. Recent studies have suggested that targeting apoE-mediated Aβ clearance may be an efficacious therapeutic strategy for reducing Aβ accumulation (50, 51). Given that LDLR has very few identified ligands compared with other apoE receptors (34), strategies aimed at modulating LDLR expression will likely be relatively specific to Aβ/apoE metabolism, presenting innovative avenues for AD prevention and treatment.

Materials and Methods

Animal Procedures. The "B" line of mice expressing the LDLR transgene (18) was cross-bred with wild-type mice and maintained on a mixed background comprising B6/C3/CBA strains. Mice overexpressing the LDLR transgene and their NTG littermates were aged to 4–5 mo for BEI experiments. Homozygous PDAPP (APPV717F) mice (background comprising DBA/2J, C57BL/6J, and Swiss Webster) were cross-bred with mice heterozygous for LDLR transgene (PD-TG). Heterozygous PDAPP mice expressing normal levels of LDLR (PD-NTG) or LDLR transgene (PD-TG) were aged to 3–4 mo or 10 mo. Comparisons between groups were made using sex-matched littermates on the same genetic background. Animal procedures were performed according to protocols accepted by the Animal Studies Committee at Washington University School of Medicine. Quantitative measurements of apoE, HJ5.1, and ISF Aβ were made using sandwich ELISAs. In vivo microdialysis (11), the BEI efflux method (15), and amyloid plaque burden analysis (18) procedures were performed as described. See *SI Materials and Methods* for further details.

Plasma Accumulation and Serial Retro-Orbital Bleeds. Plasma accumulation experiments were performed by administering 250 μg HJ5.1 (anti-$Aβ_{17–28}$ antibody generated in-house) by intrajugular injection under brief isoflurane exposure. Following injection, blood was sampled at various time points (20–240 min) by serial retro-orbital bleeding with heparinized capillary tubes (Chase Scientific Glass) under brief isoflurane exposure as described previously (30, 32). For each mouse, plasma was collected 14–16 h before injection ("prebleed") to serve as a baseline sample. Plasma was isolated by spinning blood collected in EDTA-coated microcentrifuge tubes at 7,575 × *g* at 4 °C for 9 min; plasma samples were frozen at −80 °C until measurement by mass spectrometry. For experiments in Fig. 4, plasma samples were pooled by time point in pairs (n = 12–14 mice per group) for mass spectrometry detection (n = 6–7 per group). Rates were calculated from slopes of individual linear regressions over the entire time course (n = 6–7 per group). Human Aβ was immunoprecipitated using 6E10 and quantified against a standard curve using stable isotope spike absolute quantitative (SISAQ) mass spectrometry (C2N Diagnostics). Briefly, samples were spiked with a constant vol/vol ratio of [^{15}N]-labeled Aβ40 peptide, and Aβ in the sample was immunoprecipitated using N-terminal human-specific Aβ antibody (6E10). Immunoprecipitated Aβ was trypsin-digested, and tryptic peptides were analyzed by mass spectrometry. The ratio of unlabeled to labeled $Aβ_{17–28}$ peptide was normalized against a SISAQ standard curve, allowing quantification of Aβ in the original plasma samples.

ACKNOWLEDGMENTS. We thank J. Cirrito for useful advice regarding plasma accumulation experiments; A. Sagare for radioiodination of Aβ for BEI experiments; and S. Macauley-Rambach for advice regarding BBB markers. This work was supported by National Institutes of Health Grants AG13956 and NS034467 (to D.M.H.); AG034004 (to J.M.C.); NS34467 and AG023084 (to B.V.Z.); AG029481 (to R.D.); and P30-NS057105. Support was also provided by Eli Lilly and Pfizer to Washington University in St. Louis (D.M.H.).

1. Hardy J (2006) A hundred years of Alzheimer's disease research. *Neuron* 52:3–13.
2. Golde TE, Schneider LS, Koo EH (2011) Anti-aβ therapeutics in Alzheimer's disease: The need for a paradigm shift. *Neuron* 69:203–213.
3. Benilova I, Karran E, De Strooper B (2012) The toxic Aβ oligomer and Alzheimer's disease: An emperor in need of clothes. *Nat Neurosci* 15:349–357.
4. Mawuenyega KG, et al. (2010) Decreased clearance of CNS beta-amyloid in Alzheimer's disease. *Science* 330:1774.
5. Verghese PB, Castellano JM, Holtzman DM (2011) Apolipoprotein E in Alzheimer's disease and other neurological disorders. *Lancet Neurol* 10:241–252.
6. Reiman EM, et al. (2009) Fibrillar amyloid-beta burden in cognitively normal people at 3 levels of genetic risk for Alzheimer's disease. *Proc Natl Acad Sci USA* 106:6820–6825.
7. Morris JC, et al. (2010) APOE predicts amyloid-beta but not tau Alzheimer pathology in cognitively normal aging. *Ann Neurol* 67:122–131.
8. Schmechel DE, et al. (1993) Increased amyloid beta-peptide deposition in cerebral cortex as a consequence of apolipoprotein E genotype in late-onset Alzheimer disease. *Proc Natl Acad Sci USA* 90:9649–9653.
9. Tiraboschi P, et al. (2004) Impact of APOE genotype on neuropathologic and neurochemical markers of Alzheimer disease. *Neurology* 62:1977–1983.
10. Sunderland T, et al. (2004) Cerebrospinal fluid beta-amyloid1-42 and tau in control subjects at risk for Alzheimer's disease: The effect of APOE epsilon4 allele. *Biol Psychiatry* 56:670–676.
11. Castellano JM, et al. (2011) Human apoE isoforms differentially regulate brain amyloid-β peptide clearance. *Sci Transl Med* 3:89ra57.
12. Bales KR, et al. (2009) Human APOE isoform-dependent effects on brain beta-amyloid levels in PDAPP transgenic mice. *J Neurosci* 29:6771–6779.
13. Bell RD, et al. (2007) Transport pathways for clearance of human Alzheimer's amyloid beta-peptide and apolipoproteins E and J in the mouse central nervous system. *J Cereb Blood Flow Metab* 27:909–918.
14. Deane R, et al. (2004) LRP/amyloid beta-peptide interaction mediates differential brain efflux of Abeta isoforms. *Neuron* 43:333–344.
15. Deane R, et al. (2008) apoE isoform-specific disruption of amyloid beta peptide clearance from mouse brain. *J Clin Invest* 118:4002–4013.
16. Fryer JD, et al. (2005) The low density lipoprotein receptor regulates the level of central nervous system human and murine apolipoprotein E but does not modify amyloid plaque pathology in PDAPP mice. *J Biol Chem* 280:25754–25759.
17. Cao D, Fukuchi K, Wan H, Kim H, Li L (2006) Lack of LDL receptor aggravates learning deficits and amyloid deposits in Alzheimer transgenic mice. *Neurobiol Aging* 27:1632–1643.
18. Kim J, et al. (2009) Overexpression of low-density lipoprotein receptor in the brain markedly inhibits amyloid deposition and increases extracellular A beta clearance. *Neuron* 64:632–644.
19. Katsouri L, Georgopoulos S (2011) Lack of LDL receptor enhances amyloid deposition and decreases glial response in an Alzheimer's disease mouse model. *PLoS ONE* 6:e21880.
20. Shibata M, et al. (2000) Clearance of Alzheimer's amyloid-ss(1-40) peptide from brain by LDL receptor-related protein-1 at the blood-brain barrier. *J Clin Invest* 106:1489–1499.
21. Fullerton SM, Shirman GA, Strittmatter WJ, Matthew WD (2001) Impairment of the blood-nerve and blood-brain barriers in apolipoprotein e knockout mice. *Exp Neurol* 169:13–22.
22. Methia N, et al. (2001) ApoE deficiency compromises the blood brain barrier especially after injury. *Mol Med* 7:810–815.
23. Macauley SL, Pekny M, Sands MS (2011) The role of attenuated astrocyte activation in infantile neuronal ceroid lipofuscinosis. *J Neurosci* 31(43):15575–15585.
24. Abbott NJ, Rönnbäck L, Hansson E (2006) Astrocyte-endothelial interactions at the blood-brain barrier. *Nat Rev Neurosci* 7:41–53.
25. Armulik A, et al. (2010) Pericytes regulate the blood-brain barrier. *Nature* 468(7323):557–561.
26. Yamada K, et al. (2008) The low density lipoprotein receptor-related protein 1 mediates uptake of amyloid beta peptides in an in vitro model of the blood-brain barrier cells. *J Biol Chem* 283:34554–34562.
27. Ghiso J, et al. (2004) Systemic catabolism of Alzheimer's Abeta40 and Abeta42. *J Biol Chem* 279:45897–45908.
28. Barten DM, et al. (2005) Dynamics of beta-amyloid reductions in brain, cerebrospinal fluid, and plasma of beta-amyloid precursor protein transgenic mice treated with a gamma-secretase inhibitor. *J Pharmacol Exp Ther* 312:635–643.
29. Johnson-Wood K, et al. (1997) Amyloid precursor protein processing and A beta42 deposition in a transgenic mouse model of Alzheimer disease. *Proc Natl Acad Sci USA* 94:1550–1555.
30. DeMattos RB, et al. (2001) Peripheral anti-A beta antibody alters CNS and plasma A beta clearance and decreases brain A beta burden in a mouse model of Alzheimer's disease. *Proc Natl Acad Sci USA* 98:8850–8855.
31. Seubert P, et al. (2008) Antibody capture of soluble Abeta does not reduce cortical Abeta amyloidosis in the PDAPP mouse. *Neurodegener Dis* 5:65–71.
32. DeMattos RB, Bales KR, Cummins DJ, Paul SM, Holtzman DM (2002) Brain to plasma amyloid-beta efflux: A measure of brain amyloid burden in a mouse model of Alzheimer's disease. *Science* 295:2264–2267.
33. Hardy J, Selkoe DJ (2002) The amyloid hypothesis of Alzheimer's disease: Progress and problems on the road to therapeutics. *Science* 297:353–356.
34. Bu G (2009) Apolipoprotein E and its receptors in Alzheimer's disease: pathways, pathogenesis and therapy. *Nat Rev Neurosci* 10:333–344.

35. Brown MS, Goldstein JL (1986) A receptor-mediated pathway for cholesterol homeostasis. *Science* 232:34–47.
36. Cam JA, Zerbinatti CV, Li Y, Bu G (2005) Rapid endocytosis of the low density lipoprotein receptor-related protein modulates cell surface distribution and processing of the beta-amyloid precursor protein. *J Biol Chem* 280:15464–15470.
37. Andersen OM, et al. (2005) Neuronal sorting protein-related receptor sorLA/LR11 regulates processing of the amyloid precursor protein. *Proc Natl Acad Sci USA* 102: 13461–13466.
38. Cam JA, et al. (2004) The low density lipoprotein receptor-related protein 1B retains beta-amyloid precursor protein at the cell surface and reduces amyloid-beta peptide production. *J Biol Chem* 279:29639–29646.
39. Fuentealba RA, et al. (2007) ApoER2 expression increases Abeta production while decreasing Amyloid Precursor Protein (APP) endocytosis: Possible role in the partitioning of APP into lipid rafts and in the regulation of gamma-secretase activity. *Mol Neurodegener* 2:14.
40. Kinoshita A, et al. (2001) Demonstration by fluorescence resonance energy transfer of two sites of interaction between the low-density lipoprotein receptor-related protein and the amyloid precursor protein: Role of the intracellular adapter protein Fe65. *J Neurosci* 21:8354–8361.
41. Trommsdorff M, Borg JP, Margolis B, Herz J (1998) Interaction of cytosolic adaptor proteins with neuronal apolipoprotein E receptors and the amyloid precursor protein. *J Biol Chem* 273:33556–33560.
42. Ulery PG, et al. (2000) Modulation of beta-amyloid precursor protein processing by the low density lipoprotein receptor-related protein (LRP). Evidence that LRP contributes to the pathogenesis of Alzheimer's disease. *J Biol Chem* 275: 7410–7415.
43. DeMattos RB, et al. (2004) ApoE and clusterin cooperatively suppress Abeta levels and deposition: evidence that ApoE regulates extracellular Abeta metabolism in vivo. *Neuron* 41:193–202.
44. Basak JM, Verghese PB, Yoon H, Kim J, Holtzman DM (2012) Low-density lipoprotein receptor represents an apolipoprotein E-independent pathway of Aβ uptake and degradation by astrocytes. *J Biol Chem* 287:13959–13971.
45. Yamamoto T, Choi HW, Ryan RO (2008) Apolipoprotein E isoform-specific binding to the low-density lipoprotein receptor. *Anal Biochem* 372:222–226.
46. Knouff C, et al. (2004) Defective VLDL metabolism and severe atherosclerosis in mice expressing human apolipoprotein E isoforms but lacking the LDL receptor. *Biochim Biophys Acta* 1684:8–17.
47. Bien-Ly N, Gillespie AK, Walker D, Yoon SY, Huang Y (2012) Reducing human apolipoprotein E levels attenuates age-dependent Aβ accumulation in mutant human amyloid precursor protein transgenic mice. *J Neurosci* 32:4803–4811.
48. Kim J, et al. (2011) Haploinsufficiency of human APOE reduces amyloid deposition in a mouse model of amyloid-beta amyloidosis. *J Neurosci* 31(49):18007–18012.
49. Yamada K, et al. (2009) Abeta immunotherapy: Intracerebral sequestration of Abeta by an anti-Abeta monoclonal antibody 266 with high affinity to soluble Abeta. *J Neurosci* 29:11393–11398.
50. Sadowski MJ, et al. (2006) Blocking the apolipoprotein E/amyloid-beta interaction as a potential therapeutic approach for Alzheimer's disease. *Proc Natl Acad Sci USA* 103: 18787–18792.
51. Cramer PE, et al. (2012) ApoE-directed therapeutics rapidly clear β-amyloid and reverse deficits in AD mouse models. *Science* 335:1503–1506.